

**NASA  
Technical  
Paper  
3281**

1993

# Fuel-Rich Catalytic Combustion of a High Density Fuel

Theodore A. Brabbs  
*Sverdrup Technology, Inc.*  
*Lewis Research Center Group*  
*Brook Park, Ohio*

Sylvia A. Merritt  
*Lewis Research Center*  
*Cleveland, Ohio*

**NASA**

National Aeronautics and  
Space Administration  
Office of Management  
Scientific and Technical  
Information Program



## Summary

Fuel-rich catalytic combustion (E.R. > 4) of the high-density fuel exo-tetrahydrocyclopentadiene (JP-10) was studied over the equivalence ratio range 5.0 to 7.6, which yielded combustion temperatures of 1220 to 1120 K. The process produced soot-free gaseous products similar to those obtained with iso-octane and jet-A in previous studies. The measured combustion temperature agreed well with that calculated assuming soot was not a combustion product. The process raised the effective hydrogen/carbon (H/C) ratio from 1.6 to over 2.0, thus significantly improving the combustion properties of the fuel. At an equivalence ratio near 5.0, about 80 percent of the initial fuel carbon was in light gaseous products and about 20 percent in larger condensible molecules. Fuel-rich catalytic combustion has now been studied for three fuels with H/C ratios of 2.25 (iso-octane), 1.92 (jet-A), and 1.6 (JP-10). A comparison of the product distribution of these fuels shows that, in general, the measured concentrations of the combustion products were monotonic functions of the H/C ratio with the exception of hydrogen and ethylene. In these cases, data for JP-10 fell between iso-octane and jet-A rather than beyond jet-A. It is suggested that the ring cross-linking structure of JP-10 may be responsible for this behavior. All the fuels studied showed that the largest amounts of small hydrocarbon molecules and the smallest amounts of large condensible molecules occurred at the lower equivalence ratios. This corresponds to the highest combustion temperatures used in these studies. Although higher temperatures may improve this mix, the temperature is limited. First, the life of the present catalyst would be greatly shortened when operated at temperatures of 1300 K or greater. Second, fuel-rich catalytic combustion does not produce soot because the combustion temperatures used in the experiments were well below the threshold temperature (1350 K) for the formation of soot. Increasing the temperature above this value would remove the soot-free nature of the process. Since all the fuels studied show a similar breakdown of the primary fuel into smaller molecular combustion products, this technique can be applied to all hydrocarbon fuels.

## Introduction

Fuel-rich catalytic combustion (above the normal rich limit of combustion) is a unique technique for preheating a hydrocarbon fuel to temperatures much higher than those obtained by conventional heat exchangers. In addition to producing very reactive molecules, the process upgrades the structure of the fuel by the formation of hydrogen and smaller hydrocarbon molecules. The process is soot-free and should produce a cleaner burning fuel by removing some of the fuel carbon from the soot formation mechanism chain by the formation of CO and CO<sub>2</sub>. With fuel-rich catalytic combustion as the first stage of a two-stage combustion system, these enhanced fuel properties can be utilized by engines where low emission of thermal NO<sub>x</sub> is critical and by high-speed engines where time for ignition and complete combustion is limited.

Developing hypersonic airbreathing engines with conventional fuels requires complete combustion of a hydrocarbon fuel in the supersonic flow of the combustion chamber. Since supersonic flow requires short ignition delay times and fast reaction rates, most storable liquid fuels (jet-A, for example) can not be used. However, the combustion properties of such a fuel can be enhanced to meet these requirements by the staged combustion process described previously. Recent work (refs. 1 to 3) demonstrated that fuel-rich catalytic combustion of a hydrocarbon fuel was viable. Studies with iso-octane demonstrated the feasibility of the process and work with jet-A showed that the process was viable for a conventional fuel. Jet-A was studied over the equivalence ratio range 4.6 to 7.1, which yielded combustion temperatures of 1230 to 1080 K. The process was soot-free and about 80 percent of the fuel carbon was converted to C<sub>1</sub>, C<sub>2</sub>, and C<sub>3</sub> compounds, which are known to burn adequately in a supersonic stream. The objective of the present work is to extend fuel-rich catalytic combustion to fuels used in volume-limited ramjet or scramjet applications. Since the high-density hydrocarbon exo-tetrahydrocyclopentadiene (JP-10) is a tailored fuel for missiles, a study of the ability to process this fuel in the catalytic reactor can extend the concept to this class of fuels. In addition, more information will be obtained on how the H/C ratio of a fuel affects the product distribution.

## Experimental Apparatus and Test Procedures

### Catalytic Flow-Tube Reactor

The catalytic flow-tube reactor (fig. 1) is made of two concentric tubes each approximately 2.5 m long with an inner diameter of 5 cm and an outer diameter of 11.4 cm. Although the thin-walled stainless steel inner tube was surrounded by 3.2 cm of insulation, additional external insulation was required from the air heater to the catalyst bed. Ports were available along the length of the reactor for mounting thermocouple probes, pressure probes, and the sampling probe. Two calcium fluoride windows were placed opposite each other 7.6 cm downstream of the catalyst bed so that visual or optical observations could be made of the combustion products.

### Fuel Injector

The fuel injector consisted of seven 10-cm-long conical tubes arranged with six in a circle and one in the center. Fuel was delivered to each tube through lines of equal length and of 0.04-cm inside diameter that were bent to spray the fuel in the direction of the airflow. The fuel distribution through the fuel injector was examined by measuring the flow rate of water through each of the seven fuel tubes and found to be uniform within 4 percent for all tubes. A nitrogen purge in the fuel line was required to remove any residual fuel in the fuel tubes before shutdown. This eliminated clogging of these small tubes. Figure 2 is a cross-sectional view of one of the injectors. For our test conditions the calculated drop size was about 22  $\mu\text{m}$  (ref. 4).

### Catalyst Bed

The catalyst used in these experiments was a 2:1 mixture by weight of palladium/platinum applied to cordierite honeycomb substrates coated with an alumina washcoat (information obtained in a private communication with Met-Pro Representatives, West Chester, Pa.). The total metal loading of the catalyst was 1.482  $\text{kg}/\text{m}^3$ . The substrates were 2.54 cm thick and had cell densities of 4 to 31 square cells/ $\text{cm}^2$ . To assign a numerical value to the amount of catalyst being

used, external surface areas were calculated for each size monolith as shown in table I.

### Test Procedures

Airflow through the reactor was controlled by setting the supply pressure and varying the opening of the exhaust valve at the end of the reactor. A calibrated strain gauge flowmeter measured the airflow, which was kept constant at approximately 0.4  $\text{std m}^3/\text{min}$ . The pressure at the inlet to the catalyst bed was maintained at approximately 200 kPa and the temperature was maintained at 800 K. The addition of fuel and the subsequent chemical reaction required a further adjustment of the exhaust valve to accommodate the larger gas volume produced by the changes in temperature and in the number of moles of reaction products. This venting caused the gas velocity to increase by about a factor of 3 across the 10 cm of the catalyst bed.

Standard procedures were followed for each run. These included a warmup of at least 90 minutes with hot nitrogen followed by an additional warmup of 30 to 50 minutes at the desired test conditions. This procedure produced steady-state temperatures in the reactor. The flow system was designed to permit switching the gas from nitrogen to air without interrupting the flow. Thus, the fuel flow rate could be established with hot nitrogen before switching to hot air. This ensured that the equivalence ratio in the reactor was always rich and that the catalyst never experienced a stoichiometric fuel/air condition.

### Sampling and Analysis of Product Gases

Samples were withdrawn from the reactor 17.8 cm downstream of the catalyst bed, corresponding to 15.9 to 19.5 msec of the gas-phase reaction time (dwell time). The sampling probe was a 0.33-cm-diameter stainless steel tube with three 0.06-cm-diameter holes spaced 1.3 cm apart. The three holes were positioned in the center 2.5 cm of the reactor diameter. Samples were withdrawn through heated lines into an ice-bath condenser where the liquids were trapped. The gas continued through a metal bellows type of sampling pump to a 1-liter stainless steel sampling bottle. The bottle was pressurized to about 200 kPa. A wet-test meter measured the sampling rate. At the end of a sampling run, the liquids collected in the cold trap were sealed and stored for observation. The combustion products collected in the sampling bottles were analyzed on gas chromatographs with thermal-conductivity and flame-ionization detectors. Ultra-high-purity helium was used as the carrier gas. A computing integrator determined peak areas from the detector signal. Three columns were used in analyzing the reaction product gases: washed molecular sieve, Sphercarb, and Porapak R. The external-standard method was used to determine concentrations of the species

TABLE I. — CATALYST CELL DENSITY AND SURFACE AREA

| Monolith | Cell density, cells/ $\text{cm}^2$ | Surface area, $\text{cm}^2$ |
|----------|------------------------------------|-----------------------------|
| 1        | 31.0                               | 824                         |
| 2        | 15.5                               | 549                         |
| 3        | 7.75                               | 412                         |
| 4        | 3.88                               | 282                         |

in the sample. This method compares the integrated area (signal versus time) of a standard mixture to the area of the sample. The concentration of compounds with six or more carbon atoms was determined with the C<sub>6</sub> hydrocarbon of our standard mix.

## Results and Discussion

### Fuel Vaporization

The liquid fuel must be vaporized and mixed before reaching the catalyst bed as mixing does not occur between monolith channels. In a previous report (ref. 5) it was shown that the centerline temperature 68 cm downstream of the fuel injector could be used to determine if vaporization of the fuel Jet-A was complete. Hot nitrogen gas was used for these experiments as radiation from the hot catalyst bed affected the thermocouple reading. The nitrogen is heated to about 800 K with an electric heater. The standard operating procedure was to warm the reactor for about 2 hours with hot nitrogen to attain a constant temperature profile in the reactor. Then, liquid fuel was added and the mixture was monitored 68 cm downstream of the point of fuel injection. No data were recorded until the temperature was steady for about 5 minutes. This took about 30 minutes for the first point. Then the fuel flow was increased or decreased, and additional data points were taken in the same manner. For the second point on, data could be taken every 10 minutes. The measured temperatures for JP-10/nitrogen mixtures are compared with the theoretical calculated mixture temperatures in figure 3. The range of fuel mole percent covered, from 5.5 to 10.5, resulted in a temperature drop of 240 to 340 K. The measured data show a linear decrease in temperature as the concentration of fuel increases and they are below the calculated temperature curve. This curve, the fuel/nitrogen theoretical mixture temperature versus composition, was calculated using the NASA Lewis Chemical Equilibrium Composition Program (ref. 6), and the thermodynamic data were furnished by Steele (ref. 7). The heat capacity is expressed as a fourth order polynomial

$$C_p^o = \sum_{i=1}^5 a_i T^{i-1} \quad (1)$$

and the enthalpy and entropy are calculated from  $C_p^o$  by the following relations:

$$H_T^o = a_6 + \int C_p^o dT \quad (2)$$

$$S_T^o = a_7 + \int \frac{C_p^o}{T} dT \quad (3)$$

For the assigned reference elements,

$$\Delta_f H^o(298.15) = H^o(298.15) = 0 \quad (4)$$

The coefficients of the polynomials used in the equilibrium code were obtained from the thermodynamic data with the PAC91 program (ref. 8). The vaporization coefficients for the liquid and gaseous phases of JP-10 are listed in table II.

Since fuel vaporization is an endothermic process, if the fuel is not completely vaporized, the measured temperature profile is curved and tends to stabilize to a constant temperature above the calculated curve at higher fuel concentrations. An example of this behavior is shown in figure 4, where incomplete vaporization of iso-octane occurred. Note the leveling off of the temperature to values well above the theoretical mixture temperature. Figure 5 shows the same iso-octane/nitrogen mixture temperatures measured using an improved fuel injector (ref. 4) which yielded completely (or almost completely) vaporized data. The observed difference between the calculated mixture temperatures and the measured ones can be attributed to the apparatus heat losses for a nonadiabatic system. The system was calibrated by plotting the difference between the measured and calculated temperatures as a function of the temperature. This calibration can be used to correct the experimental data of other fuels for the apparatus heat losses. The JP-10 raw data corrected for heat loss along the drift tube are shown in figure 6. The comparison of the corrected measured temperatures with the calculated mixture vaporization temperatures are relatively close in magnitude and have a similar profile. The appearance of the present data strongly suggests that the fuel is completely vaporized and that we are measuring an equilibrium temperature.

### Combustion of JP-10

Fuel-rich catalytic combustion of the high-density fuel JP-10 was highly successful. The fuel was studied over the equivalence ratio range 5.0 to 7.6 with combustion temperatures ranging from 1220 to 1120 K. Flashback and spontaneous ignition of the fuel were not problems for the test conditions

TABLE II. - JP-10 VAPORIZATION COEFFICIENTS

| Vaporization coefficient | Liquid          | Gas             |
|--------------------------|-----------------|-----------------|
| a <sub>1</sub>           | 1.90149323E+01  | 2.31301566E+01  |
| a <sub>2</sub>           | -8.45303904E-02 | -1.30608922E-01 |
| a <sub>3</sub>           | 6.72215359E-04  | 5.77711149E-04  |
| a <sub>4</sub>           | -1.23077905E-06 | -6.34792880E-07 |
| a <sub>5</sub>           | 7.95025458E-10  | 1.90996886E-10  |
| a <sub>6</sub>           | -2.05333989E+04 | -1.38995270E+04 |
| a <sub>7</sub>           | -6.76301742E+01 | -6.39418369E+01 |

used in the present study. In the study with jet-A fuel a poor fuel injector resulted in spontaneous ignition in the mixing section. This event caused a large amount of soot to form and the combustion products observed through the window downstream of the catalyst were completely opaque. Thus, for the equivalence ratio used in the present study, if soot forms one expects to see opaque gases through the observation window. In the present experiments the gaseous products observed through the windows were completely transparent for all test conditions, indicating that the process was soot-free.

The reaction temperature was measured 3.8 cm downstream of the catalyst with a shielded closed-end thermocouple. Figure 7 is a plot of the measured reaction temperatures versus equivalence ratio. These measured temperatures were compared with equilibrium combustion temperatures calculated by assuming that soot was or was not a product. The measured temperatures are in good agreement with the

line calculated for no soot. This was the same behavior observed for the fuels iso-octane and jet-A (ref. 9, fig. 3).

Table III shows a comparison of the reaction products, temperatures, and equivalence ratios for the gas samples taken in the present study. The products are divided into two groups as was done in the previous studies. Group 1 contains  $H_2$ ,  $O_2$ ,  $N_2$ , and all  $C_1$  and  $C_2$  carbon-containing compounds while group 2 contains the larger hydrocarbons. The gas analysis shows that the breakdown of JP-10 is similar to that of iso-octane and jet-A.

In addition to the measured gaseous products, condensible reaction products were collected in the ice-bath cold trap. The condensibles are large carbon-containing molecules which are volatile in the high temperature atmosphere of the reactor but readily condense when cooled to the trap temperature. The condensibles are soluble in acetone and unstable even at room temperature. Slow reaction at room temperature caused the condensibles to change in color

TABLE III. — JP-10 GASEOUS REACTION PRODUCTS

|                         |       |       |       |       |       |       |       |
|-------------------------|-------|-------|-------|-------|-------|-------|-------|
| Reaction temperature, K | 1220  | 1201  | 1164  | 1155  | 1149  | 1135  | 1122  |
| Equivalence ratio       | 5.06  | 5.46  | 6.23  | 6.94  | 6.10  | 7.08  | 7.58  |
| Fuel flow, g mole/min   | 0.865 | 0.992 | 0.989 | 1.124 | 0.883 | 1.045 | 1.099 |
| Air flow, g mole/min    | 11.43 | 11.27 | 10.61 | 10.82 | 9.67  | 9.87  | 9.68  |
| Pressure, kPa:          |       |       |       |       |       |       |       |
| Upstream                | 22.30 | 22.34 | 22.69 | 22.61 | 23.69 | 23.68 | 23.67 |
| Downstream              | 22.30 | 22.35 | 22.71 | 22.63 | 23.67 | 23.67 | 23.64 |
| $\Delta P$ across bed   | 0.00  | 0.01  | 0.02  | 0.02  | 0.02  | 0.01  | 0.03  |
| Temperature, K:         |       |       |       |       |       |       |       |
| Preheated air           | 794   | 794   | 795   | 797   | 791   | 792   | 790   |
| Fuel                    | 302   | 302   | 301   | 300   | 304   | 302   | 303   |
| Group 1:                |       |       |       |       |       |       |       |
| Hydrogen                | 8.07  | 7.35  | 6.75  | 6.03  | 6.89  | 5.74  | 5.45  |
| Oxygen                  | 1.38  | 1.50  | 1.87  | 1.79  | 1.55  | 1.49  | 1.69  |
| Nitrogen                | 60.79 | 61.26 | 61.93 | 63.56 | 61.44 | 64.31 | 65.11 |
| Carbon monoxide         | 14.70 | 13.33 | 11.62 | 10.57 | 11.65 | 9.55  | 9.36  |
| Carbon dioxide          | 3.37  | 3.66  | 4.27  | 4.82  | 4.57  | 5.12  | 5.47  |
| Methane                 | 2.88  | 2.56  | 2.18  | 1.61  | 2.25  | 1.53  | 1.34  |
| Acetylene               | 0.73  | 0.48  | 0.31  | 0.18  | 0.34  | 0.17  | 0.12  |
| Ethylene                | 4.24  | 4.67  | 6.00  | 4.64  | 5.81  | 5.82  | 4.91  |
| Ethane                  | ---   | 0.07  | 0.11  | 0.11  | 0.11  | 0.10  | 0.11  |
| Total                   | 96.15 | 94.87 | 95.04 | 93.30 | 94.62 | 93.82 | 93.56 |
| Group 2:                |       |       |       |       |       |       |       |
| Propylene               | 0.31  | 0.58  | 0.91  | 1.10  | 0.88  | 1.17  | 1.23  |
| C3 hydrocarbons         | 0.15  | 0.16  | 0.14  | 0.10  | 0.14  | 0.09  | 0.08  |
| C4 hydrocarbons         | 0.27  | 0.41  | 0.58  | 0.69  | 0.52  | 0.67  | 0.68  |
| C5 hydrocarbons         | 0.07  | 0.16  | 0.80  | 0.67  | 0.38  | 0.43  | 0.56  |
| C6 hydrocarbons         | ---   | ---   | ---   | 0.11  | ---   | 0.10  | 0.14  |
| Benzene                 | 1.65  | 1.98  | 1.61  | 1.54  | 1.34  | 1.33  | 1.14  |
| Toluene                 | 0.52  | 0.69  | 0.71  | 0.88  | 0.55  | 0.57  | 0.64  |
| C7 hydrocarbon          | ---   | ---   | ---   | 0.00  | ---   | 0.00  | 0.01  |
| Styrene                 | 0.03  | 0.03  | 0.01  | 0.01  | 0.01  | 0.01  | 0.01  |
| C8 hydrocarbons         | 0.02  | 0.02  | 0.01  | 0.39  | 0.02  | 0.02  | -0.02 |
| Total                   | 3.03  | 4.03  | 4.78  | 5.49  | 3.85  | 4.38  | 4.52  |
| Total (groups 1 and 2)  | 99.18 | 98.90 | 99.81 | 98.80 | 98.47 | 98.20 | 98.09 |

from yellow-brown to black. This was observed even in a nitrogen atmosphere. No attempt was made to analyze the condensible products.

The carbon-atom balance across the catalyst bed was calculated from the measured reaction products. Changes in the number of moles due to chemical reaction were accounted for by using nitrogen as a reference gas and calculating the carbon-nitrogen ratio before and after the catalyst bed. Figure 8 is a plot of the percentage of initial fuel carbon found in the product gases as a function of the equivalence ratio. Any carbon not accounted for in the product gas was believed to be contained in the large-molecular compounds which condensed in the cold trap.

Fuel-rich catalytic combustion enhances the fuel's combustion properties by forming hydrogen and smaller hydrocarbons and removes some of the fuel carbon from the soot formation process. This carbon removal is accomplished by the formation of carbon monoxide and carbon dioxide, both of

which are known not to form soot at the combustion temperatures of a hydrocarbon fuel. The effective H/C ratio of the processed fuel was calculated by subtracting the amount of carbon in carbon monoxide and carbon dioxide from the total fuel carbon and dividing the initial hydrogen by the balance of the carbon. Figure 9 shows the increase in this ratio by the process.

### Effect of Hydrogen/Carbon Ratio

Three fuels have now been studied to show the practicality of catalytically burning a fuel in a fuel-rich environment (E.R. > 4) without the formation of soot. These fuels are iso-octane (ref. 2), jet-A (ref. 3), and JP-10 where the hydrogen/carbon ratios are 2.25, 1.92 and 1.60, respectively. Comparisons of these fuels can be made by comparing tables III, IV, and V, which show the reaction products,

TABLE IV. - JET-A GASEOUS REACTION PRODUCTS<sup>a</sup>

|                         |        |        |        |        |        |        |        |       |       |
|-------------------------|--------|--------|--------|--------|--------|--------|--------|-------|-------|
| Reaction temperature, K | 1228   | 1213   | 1202   | 1190   | 1166   | 1146   | 1124   | 1107  | 1083  |
| Equivalence ratio       | 4.60   | 4.76   | 4.91   | 5.02   | 5.25   | 5.68   | 6.16   | 6.52  | 7.07  |
| Fuel flow, g mole/min   | 0.580  | 0.602  | 0.623  | 0.646  | 0.757  | 0.823  | 0.895  | 0.958 | 1.037 |
| Air flow, g mole/min    | 10.68  | 10.73  | 10.76  | 10.89  | 12.22  | 12.28  | 12.32  | 12.46 | 12.44 |
| Pressure, kPa:          |        |        |        |        |        |        |        |       |       |
| Upstream                | 156.70 | 156.00 | 156.40 | 155.80 | 160.30 | 159.70 | 159.00 | 159.2 | 159.4 |
| Downstream              | 156.40 | 155.80 | 156.20 | 155.70 | 159.70 | 159.30 | 158.80 | 159.2 | 158.5 |
| ΔP across bed           | 0.30   | 0.20   | 0.20   | 0.10   | 0.60   | 0.40   | 0.20   | 0.00  | 0.90  |
| Temperature, K:         |        |        |        |        |        |        |        |       |       |
| Preheated air           | 799    | 799    | 800    | 800    | 800    | 801    | 801    | 803   | 803   |
| Fuel                    | 302    | 302    | 301    | 301    | 304    | 303    | 303    | 302   | 301   |
| Group 1:                |        |        |        |        |        |        |        |       |       |
| Hydrogen                | 7.70   | 7.23   | 6.83   | 6.26   | 5.58   | 4.76   | 3.92   | 3.43  | 2.83  |
| Oxygen                  | 0.89   | 0.91   | 0.96   | 0.99   | 1.05   | 1.03   | 1.13   | 1.22  | 1.4   |
| Nitrogen                | 59.76  | 58.85  | 59.68  | 59.05  | 59.90  | 60.43  | 59.80  | 61.68 | 63.15 |
| Carbon monoxide         | 16.84  | 16.47  | 15.94  | 15.74  | 15.02  | 13.89  | 12.39  | 11.96 | 10.94 |
| Carbon dioxide          | 2.21   | 2.18   | 2.20   | 2.27   | 2.29   | 2.61   | 5.47   | 3.23  | 3.49  |
| Methane                 | 5.34   | 5.34   | 5.41   | 5.32   | 4.91   | 4.58   | 1.34   | 3.71  | 3.32  |
| Acetylene               | 1.134  | 1.000  | 0.877  | 0.731  | 0.360  | 0.237  | 0.12   | 0.124 | 0.076 |
| Ethylene                | 5.34   | 5.81   | 6.53   | 6.56   | 7.02   | 7.57   | 4.91   | 7.61  | 6.76  |
| Ethane                  | 0.09   | 0.13   | 0.16   | 0.21   | 0.38   | 0.47   | 0.11   | 0.64  | 0.59  |
| Total                   | 99.30  | 97.92  | 98.59  | 97.13  | 96.51  | 95.58  | 93.56  | 93.60 | 92.56 |
| Group 2:                |        |        |        |        |        |        |        |       |       |
| Propylene               | 0.17   | 0.25   | 0.32   | 0.47   | 1.23   | 1.77   | 1.23   | 2.44  | ---   |
| C3 hydrocarbons         | 0.133  | 0.155  | 0.171  | 0.189  | 0.191  | 0.162  | 0.08   | 0.058 | ---   |
| C4 hydrocarbons         | 0.17   | 0.21   | 0.25   | 0.32   | 0.74   | 1.14   | 0.68   | 1.59  | ---   |
| C5 hydrocarbons         | 0.04   | 0.05   | 0.06   | 0.07   | 0.16   | 0.28   | 0.56   | 0.56  | ---   |
| C6 hydrocarbons         | 0.002  | 0.003  | 0.003  | 0.000  | 0.004  | 0.026  | 0.14   | 0.110 | ---   |
| Benzene                 | 0.48   | 0.47   | 0.53   | 0.50   | 0.43   | 0.42   | 1.14   | 0.34  | ---   |
| Toluene                 | 0.22   | 0.23   | 0.31   | 0.29   | 0.27   | 0.31   | 0.64   | 0.32  | ---   |
| C7 hydrocarbon          | 0.000  | 0.000  | 0.000  | 0.000  | 0.000  | 0.005  | 0.01   | 0.027 | ---   |
| Styrene                 | 0.040  | 0.040  | 0.063  | 0.043  | 0.030  | 0.011  | 0.01   | 0.011 | ---   |
| C8 hydrocarbons         | 0.021  | 0.023  | 0.033  | 0.025  | 0.038  | 0.029  | 0.02   | 0.061 | ---   |
| Total                   | 1.28   | 1.43   | 1.74   | 1.91   | 3.09   | 4.15   | 4.52   | 5.52  | ---   |
| Total (groups 1 and 2)  | 100.58 | 98.90  | 100.33 | 99.04  | 99.60  | 99.73  | 98.09  | 97.31 | ---   |

<sup>a</sup>Reference 9.

TABLE V. — ISO-OCTANE GASEOUS REACTION PRODUCTS<sup>a</sup>

|                         |        |        |        |        |        |
|-------------------------|--------|--------|--------|--------|--------|
| Reaction temperature, K | 1200   | 1170   | 1138   | 1114   | 1093   |
| Equivalence ratio       | 4.80   | 5.50   | 6.56   | 7.22   | 7.87   |
| Fuel flow, g mole/min   | 1.266  | 1.465  | 1.751  | 1.937  | 2.099  |
| Air flow, g mole/min    | 15.75  | 15.89  | 15.93  | 16.00  | 15.92  |
| Pressure, kPa:          |        |        |        |        |        |
| Upstream                | 198.40 | 197.40 | 197.30 | 198.50 | 198.60 |
| Downstream              | 196.70 | 197.40 | 196.70 | 197.60 | 197.80 |
| ΔP across bed           | 1.7    | 0.0    | 0.6    | 0.9    | 0.8    |
| Temperature, K:         |        |        |        |        |        |
| Preheated air           | 815    | 813    | 815    | 813    | 811    |
| Fuel                    | 549    | 532    | 508    | 491    | 476    |
| Group 1:                |        |        |        |        |        |
| Hydrogen                | 12.54  | 12.11  | 8.28   | 5.84   | 4.58   |
| Oxygen                  | 0.73   | 0.75   | 0.79   | 0.87   | 0.92   |
| Nitrogen                | 53.23  | 53.10  | 55.86  | 58.14  | 59.93  |
| Carbon monoxide         | 17.41  | 16.32  | 13.28  | 11.49  | 10.33  |
| Carbon dioxide          | 1.78   | 2.07   | 2.68   | 3.10   | 3.37   |
| Methane                 | 6.34   | 5.83   | 6.12   | 5.71   | 4.91   |
| Acetylene               | 0.15   | 0.08   | 0.06   | 0.03   | 0.04   |
| Ethylene                | 4.08   | 3.21   | 4.20   | 3.29   | 2.00   |
| Ethane                  | 0.42   | 0.50   | 0.59   | 0.51   | 0.48   |
| Total                   | 96.68  | 93.97  | 91.86  | 88.98  | 86.56  |
| Group 2:                |        |        |        |        |        |
| Propylene               | 1.66   | 2.57   | 3.61   | 4.13   | 4.13   |
| Allene                  | 0.24   | 0.25   | 0.22   | 0.16   | 0.13   |
| Methyl acetylene        | 0.20   | 0.16   | 0.12   | 0.10   | 0.10   |
| C4 hydrocarbons         | 1.42   | 2.77   | 4.05   | 5.59   | 6.17   |
| C5 hydrocarbons         | 0.06   | 0.23   | 0.48   | 0.91   | 0.95   |
| Benzene                 | 0.12   | 0.09   | 0.10   | 0.09   | 0.09   |
| Toluene                 | 0.03   | 0.03   | 0.04   | 0.21   | 0.00   |
| Iso-octane              | 0.00   | 0.03   | 0.24   | 0.89   | 2.04   |
| Total                   | 3.73   | 6.13   | 8.86   | 12.08  | 13.61  |
| Total (groups 1 and 2)  | 100.58 | 100.10 | 100.72 | 101.06 | 100.17 |

<sup>a</sup>Reference 2.

combustion temperature, and equivalence ratios for the three fuels.

The concentration of hydrogen in the product gas can be seen in figure 10(a). The maximum hydrogen concentrations are obtained at an equivalence ratio (E.R.) equal to the minimum values tested for all three fuels. This is followed by a steady decrease in concentration as the equivalence ratio increases. The data for iso-octane (2.25) and jet-A (1.92) scale with the H/C ratio-iso-octane yielding the most hydrogen and JP-10 falling in between the two fuels. Although it is not presently clear why JP-10 behaves as it does, we suspect that the ring cross-linking structure of the fuel (see fig. 11) may be responsible for the behavior.

An interesting observation is made in figure 10(b) where the sum of carbon monoxide and carbon dioxide concentrations are plotted versus the equivalence ratio. For all three fuels the concentrations of these gases are about the same and show no dependence on the H/C ratio of the fuel. This

suggests that the mechanism leading to the formation of these products is independent of the type of hydrocarbon present. The maximum carbon monoxide and carbon dioxide concentration was at the lowest equivalence ratios studied. This is followed by a gradual decay as the equivalence ratio increases.

Saturated molecules such as methane can be observed in figure 10(c), where the concentration of the saturated molecules in the product gas is plotted versus equivalence ratio. We can see that for all three fuels the concentrations decrease steadily as equivalence ratio increases. The maximum methane concentration observed in the product gas was at the minimum equivalence ratio tested for all of the fuels. In this case, the concentrations do scale with the H/C ratio, iso-octane being the highest and JP-10 the lowest.

Ethylene is an example of an unsaturated compound. Its concentration in the product gases is shown in figure 10(d) where the percent ethylene is plotted versus the equivalence ratio. Unlike the other products discussed, the ethylene concentration first increased and then decreased as the equivalence ratio is increased. Maximum concentrations occur between an equivalence ratio of 6 to 7 for all fuels studied. Similar to the behavior of hydrogen already discussed, the percent ethylene in the product gases for iso-octane and jet-A scale with the H/C ratio but the data for JP-10 plots between the two fuels.

Figure 12(a) is a plot of the percentage of initial fuel carbon found in the measured product gases as a function of the equivalence ratio. The calculation of the carbon-atom balance across the catalyst bed was discussed in a previous section. At an equivalence ratio near 5, the gas analysis showed that 100 percent of the fuel carbon was recovered in the gas sample for H/C = 2.25 (iso-octane) while only about 80 percent of the fuel was in the gas sample for H/C = 1.6 (JP-10). The balance of the fuel carbon for jet-A and JP-10 were in molecules too large to pass through the ice-bath cold trap. With the exception of iso-octane, increasing the equivalence ratio resulted in an increase in the percent of condensible hydrocarbons. However, in the case of iso-octane, table V shows that at high equivalence ratios some of the initial fuel was unreacted downstream of the catalyst bed. Thus, the increase in condensibles for jet-A and JP-10 may also have been due to unreacted fuel.

Figure 12(b) shows the percentage of the fuel carbon converted to C<sub>1</sub>, C<sub>2</sub>, and C<sub>3</sub> compounds for the three fuels. These values were calculated by the same method used for the carbon-atom balance. The maximum values obtained for the three fuels range from 95 to 55 percent, iso-octane being the largest and JP-10 the lowest. The tendency to converge at higher equivalence ratios (E.R. = 4 to 5) demonstrates the need for higher temperatures to more completely break up the large fuel molecules.

## Summary of Results

Fuel-rich catalytic combustion of the high-density fuel *exo*-tetrahydrocyclopentadiene (JP-10) was studied over the equivalence ratio range of 5.0 to 7.6 resulted in combustion temperatures of 1220 to 1120 K. The process which was highly successful with this fuel, produced soot-free gaseous products similar to those obtained with the previous fuels studied. Near an equivalence ratio of 5, 80 percent of the initial fuel carbon was in gaseous products and 20 percent in larger condensible molecules. The measured combustion temperatures agreed well with those calculated assuming soot was not a combustion product. The process raised the H/C ratio from 1.6 to over 2.0, thus significantly improving the combustion properties of the fuel. Fuel-rich catalytic combustion has now been studied for three fuels — iso-octane (2.25), jet-A (1.92), and JP-10 (1.6). A comparison of the product distribution of these fuels shows that, in general, the measured combustion products changed monotonically with the H/C ratio with the exception of hydrogen and ethylene. In these cases, data for JP-10 fell between iso-octane and jet-A rather than beyond jet-A. It is suggested that the ring cross-linking structure of JP-10 may be responsible for this behavior. All the fuels studied showed that the largest amounts of small hydrocarbon molecules and the smallest amounts of large condensible molecules occurred at the lower equivalence ratios. This finding corresponds to the highest combustion temperatures used in these studies. Although higher temperatures may improve this mix, the temperature is limited. First, the life of the present catalyst would be greatly shortened when operated at temperatures of 1300 K or greater. Second, fuel-rich catalytic combustion does not produce soot because the combustion temperatures used in the experiments were well below the threshold

temperature (1350 K) for the formation of soot (ref. 1). Increasing the temperature above this value would remove the soot-free nature of the process. Since all the fuels studied showed a similar breakdown of the primary fuel into smaller combustion products, this technique should be applicable to all hydrocarbon fuels.

## References

1. Gomez, A.; Littman, M.G.; and Glassman, I.: Comparative Study of Soot Formation on the Centerline of Axisymmetric Laminar Diffusion Flames: Fuel and Temperature Effects. *Combust. Flame*, vol. 70, 1987, pp. 225-241 (1987).
2. Brabbs, T.A.; and Olson, S.L.: Fuel-Rich Catalytic Combustion — A Soot Free Technique for In Situ Hydrogen-Like Enrichment. NASA TP-2498, 1985.
3. Brabbs, T.A.; Gracia-Salcedo, C.M.: Fuel-Rich Catalytic Combustion of Jet-A Fuel — Equivalence Ratios 5.0 to 8.0. NASA TM-101975, 1989.
4. Gracia-Salcedo, C. M.: Experimental Study of the Vaporization of Jet-A Fuel. M.S. Thesis, Case Western Reserve University, Cleveland, OH, 1989.
5. Gracia-Salcedo, C.M.; Brabbs, T.A.; and McBride, B.J.: Experimental Verification of the Thermodynamic Properties for a Jet-A Fuel. NASA TM-101475, 1988.
6. Gordon, S.; and McBride, B.J.: Computer Program for Calculation of Complex Chemical Equilibrium Compositions, Rocket Performance, Incident and Reflected Shocks, and Chapman-Juguet Detonations. NASA SP-273, 1976.
7. Steele W.V.; and Chirico R.D.: Accurate Measurement of Thermochemical and Thermophysical Properties of Future Jet Fuels. Symposium on the Structure of Future Jet Fuels II, American Chemical Society, 1989, pp. 876-884.
8. McBride, B.J.; and Gordon, S.: Computer Program for Calculating and Fitting Thermodynamic Functions. NASA RP-1271, 1992.
9. Brabbs, T.A.; Rollbuhler, R.J.; and Lezberg, E. A.: Fuel-Rich Catalytic Combustion — A Fuel Processor for High Speed Propulsion. NASA TM-103177, 1990.

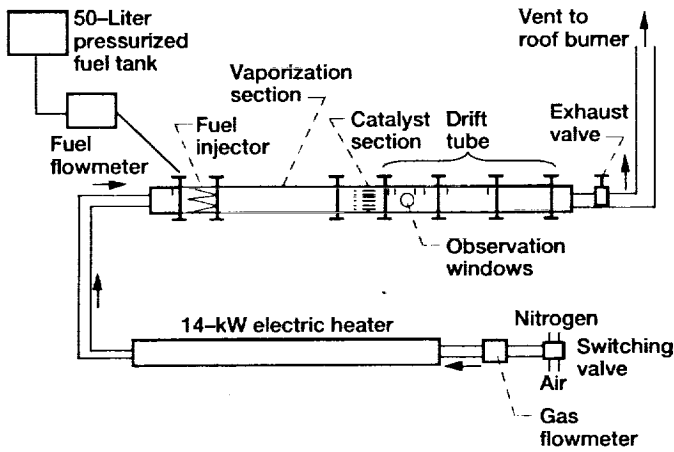


Figure 1.—Schematic drawing of test apparatus.

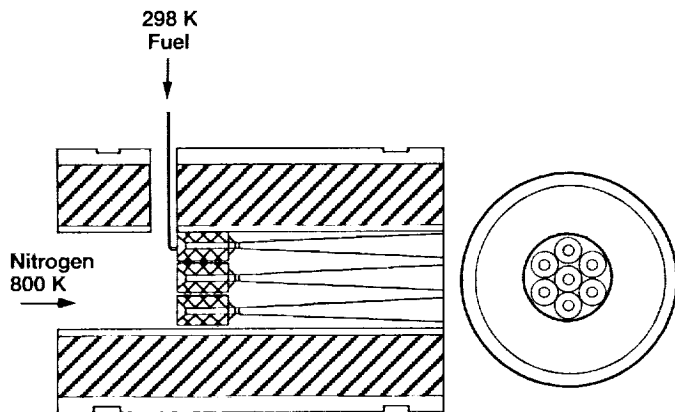


Figure 2.—Sketch of side and end views of fuel injector section.

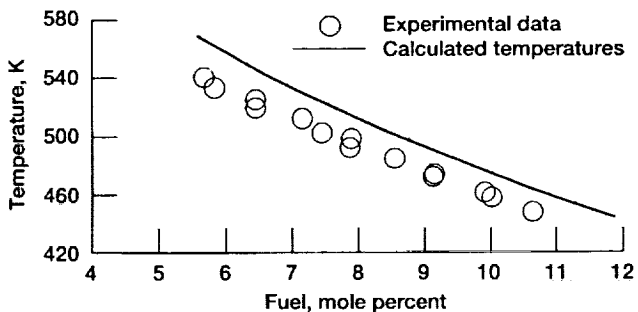


Figure 3.—Comparison of measured temperatures of vaporized JP-10/nitrogen mixtures and calculated equilibrium temperatures for the mix. Note that character of data is similar to that of calculated curve. This is a strong indication of complete fuel vaporization.

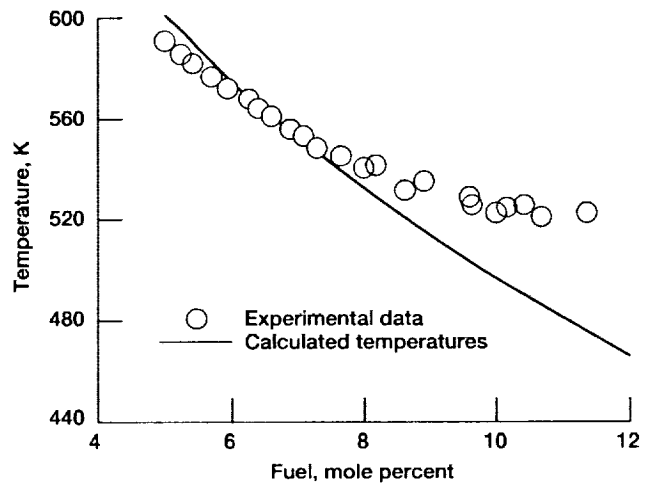


Figure 4.—Measured temperatures of iso-octane/nitrogen mixtures showing effect of incomplete vaporization (ref. 7, fig. 2).

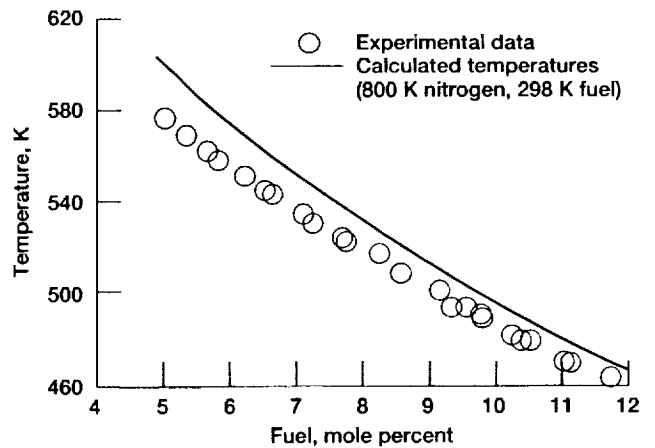


Figure 5.—Measured temperatures of iso-octane/nitrogen mixtures using fuel injector B. Note that character of data is similar to that of calculated curve. This is a strong indication of complete fill vaporization. Small difference in temperatures can be attributed to apparatus heat loss.

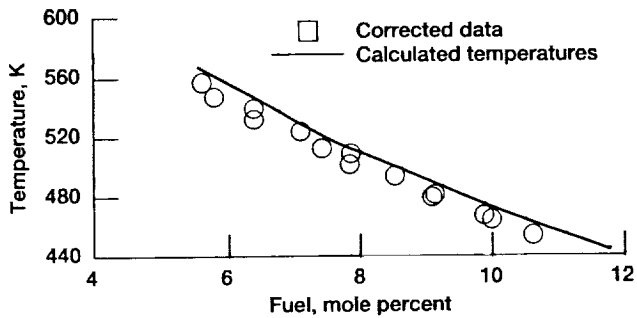


Figure 6.—Experimental JP-10 data corrected for apparatus heat loss.

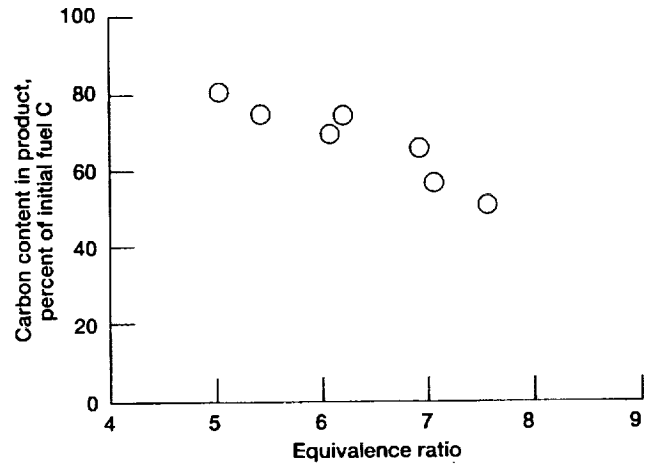


Figure 8.—Percent initial fuel carbon to product gases for JP-10 fuel as function of equivalence ratio, calculated using carbon/nitrogen ratio before and after catalyst bed.

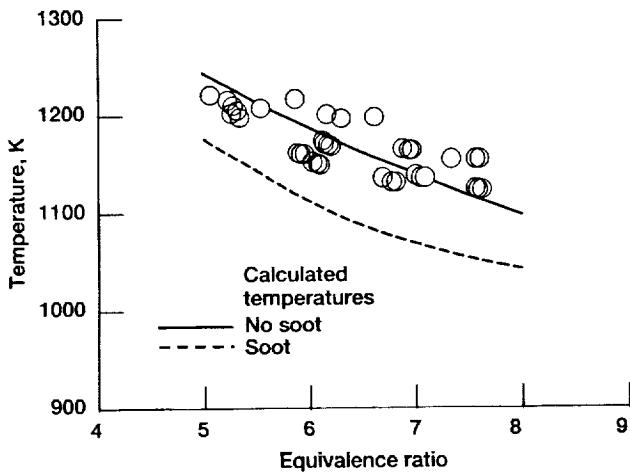


Figure 7.—Comparison of JP-10 measured reaction temperatures with calculated equilibrium temperatures (with and without soot).

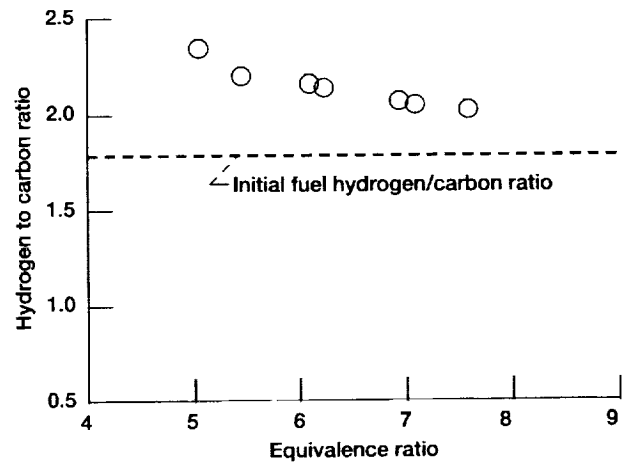


Figure 9.—Effect of removing some of (JP-10) fuel carbon from soot formation chain.

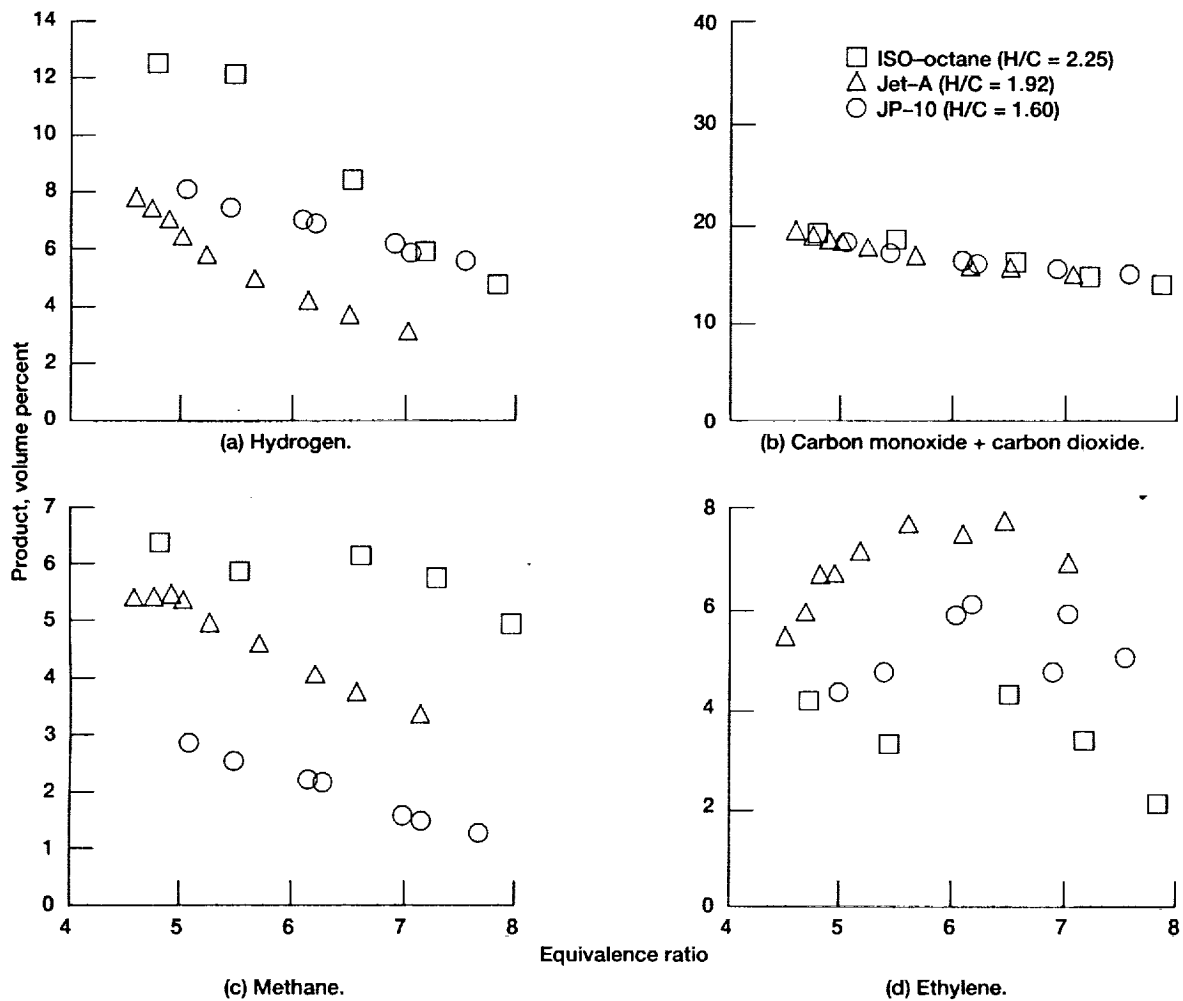


Figure 10.—Comparison of some reaction products as functions of equivalence ratio for three fuels studied.

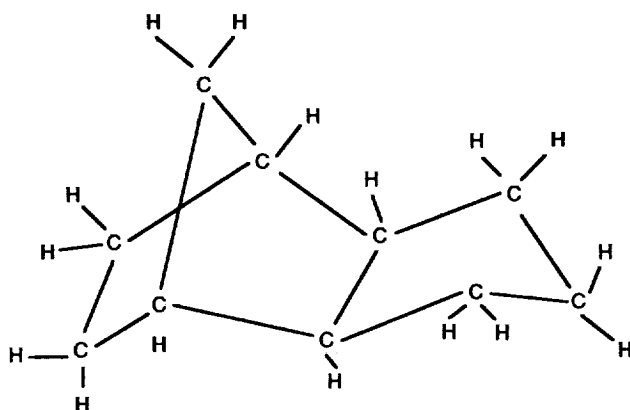
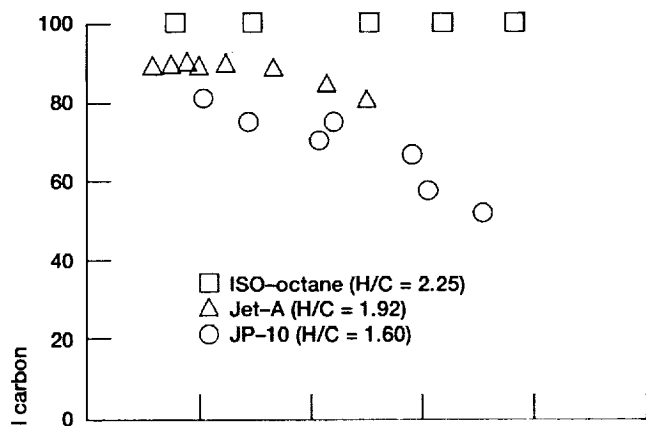
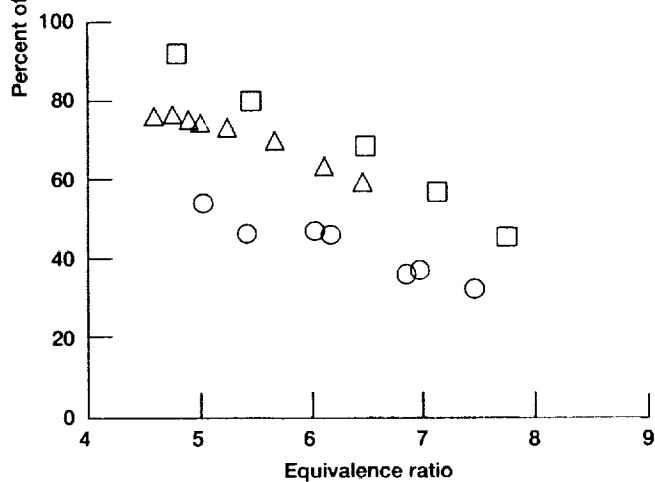


Figure 11.—Schematic diagram of bridged-ring structure of JP-10 (exo-tetrahydrodicyclopentadiene).



(a) Initial fuel carbon in product gas.



(b) Carbon converted to C1, C2, and C3 compounds.

Figure 12.—Percentage of fuel carbon measured in collected gas samples as function of equivalence ratio for three fuels.



| REPORT DOCUMENTATION PAGE   |  |  | Form Approved<br>OMB No. 0704-0188 |  |
|---|--|--|------------------------------------|--|
| Public reporting burden for this collection of information is estimated to average 1 hour per response, including the time for reviewing instructions, searching existing data sources, gathering and maintaining the data needed, and completing and reviewing the collection of information. Send comments regarding this burden estimate or any other aspect of this collection of information, including suggestions for reducing this burden, to Washington Headquarters Services, Directorate for Information Operations and Reports, 1215 Jefferson Davis Highway, Suite 1204, Arlington, VA 22202-4302, and to the Office of Management and Budget, Paperwork Reduction Project (0704-0188), Washington, DC 20503.  |  |  |                                    |  |
| 1. AGENCY USE ONLY (Leave blank)  | 2. REPORT DATE<br>July 1993                              | 3. REPORT TYPE AND DATES COVERED<br>Technical Paper  |                                    |  |
| 4. TITLE AND SUBTITLE<br>Fuel-Rich Catalytic Combustion of a High Density Fuel  |  | 5. FUNDING NUMBERS<br><br>WU-505-62-52   |                                    |  |
| 6. AUTHOR(S)<br>Theodore A. Brabbs and Sylvia A. Merritt  |  | 7. PERFORMING ORGANIZATION NAME(S) AND ADDRESS(ES)<br>National Aeronautics and Space Administration<br>Lewis Research Center<br>Cleveland, Ohio 44135-3191   |                                    |  |
| 8. PERFORMING ORGANIZATION REPORT NUMBER<br><br>E-7298  |  | 9. SPONSORING/MONITORING AGENCY NAMES(S) AND ADDRESS(ES)<br>National Aeronautics and Space Administration<br>Washington, D.C. 20546-0001   |                                    |  |
| 10. SPONSORING/MONITORING AGENCY REPORT NUMBER<br><br>NASA TP-3281  |  | 11. SUPPLEMENTARY NOTES<br>Theodore A. Brabbs, Sverdrup Technology, Inc., Lewis Research Center Group, 2001 Aerospace Parkway, Brook Park, Ohio 44142 and Sylvia A. Merritt, NASA Lewis Research Center. Responsible person, Theodore A. Brabbs, (216) 433-5839. |                                    |  |
| 12a. DISTRIBUTION/AVAILABILITY STATEMENT<br><br>Unclassified - Unlimited<br>Subject Category 25   |  | 12b. DISTRIBUTION CODE   |                                    |  |
| 13. ABSTRACT (Maximum 200 words)<br><br>Fuel-rich catalytic combustion (E.R. > 4) of the high-density fuel exo-tetrahydrocyclopentadiene (JP-10) was studied over the equivalence ratio range 5.0 to 7.6, which yielded combustion temperatures of 1220 to 1120 K. The process produced soot-free gaseous products similar to those obtained with iso-octane and jet-A in previous studies. The measured combustion temperature agreed well with that calculated assuming soot was not a combustion product. The process raised the effective hydrogen/carbon (H/C) ratio from 1.6 to over 2.0, thus significantly improving the combustion properties of the fuel. At an equivalence ratio near 5.0, about 80 percent of the initial fuel carbon was in light gaseous products and about 20 percent in larger condensible molecules. Fuel-rich catalytic combustion has now been studied for three fuels with H/C ratios of 2.25 (iso-octane), 1.92 (jet-A), and 1.6 (JP-10). A comparison of the product distribution of these fuels shows that, in general, the measured concentrations of the combustion products were monotonous functions of the H/C ratio with the exception of hydrogen and ethylene. In these cases, data for JP-10 fell between iso-octane and jet-A rather than beyond jet-A. It is suggested that the ring cross-linking structure of JP-10 may be responsible for this behavior. All the fuels studied showed that the largest amounts of small hydrocarbon molecules and the smallest amounts of large condensible molecules occurred at the lower equivalence ratios. This corresponds to the highest combustion temperatures used in these studies. Although higher temperatures may improve this mix, the temperature is limited. First, the life of the present catalyst would be greatly shortened when operated at temperatures of 1300 K or greater. Second, fuel-rich catalytic combustion does not produce soot because the combustion temperatures used in the experiments were well below the threshold temperature (1350 K) for the formation of soot. Increasing the temperature above this value would remove the soot-free nature of the process. Since all of the fuels studied show a similar breakdown of the primary fuel into smaller molecular combustion products this technique can be applied to all hydrocarbon fuels. |  |  |                                    |  |
| 14. SUBJECT TERMS<br>Catalytic combustion; JP-10 fuel; Fuel-rich combustion; Soot-free combustion; Soot precursor; High temperature fuel; Preheat technique   |  |  | 15. NUMBER OF PAGES<br>16          |  |
|   |  |  | 16. PRICE CODE<br>A03              |  |
| 17. SECURITY CLASSIFICATION OF REPORT<br>Unclassified   | 18. SECURITY CLASSIFICATION OF THIS PAGE<br>Unclassified | 19. SECURITY CLASSIFICATION OF ABSTRACT<br>Unclassified  | 20. LIMITATION OF ABSTRACT         |  |

